Kinetic Study of Scale Inhibitor Precipitation in Squeeze Treatment

ARTICLE *in* CRYSTAL GROWTH & DESIGN · DECEMBER 2004

Impact Factor: 4.89 · DOI: 10.1021/cg049874d

4 AUTHORS, INCLUDING:

H.s. Fogler
University of Michigan
284 PUBLICATIONS **7,989** CITATIONS

SEE PROFILE

CRYSTAL GROWTH & DESIGN
2005
VOL. 5, NO. 1
329−335

Kinetic Study of Scale Inhibitor Precipitation in Squeeze Treatment

V. Tantayakom,[†,‡] H. S. Fogler,[*,†] P. Charoensirithavorn,[‡] and S. Chavadej[‡]

Department of Chemical Engineering, University of Michigan, Ann Arbor, Michigan 48109, and The Petroleum and Petrochemical College, Chulalongkorn University, Bangkok, Thailand

Received April 3, 2004; Revised Manuscript Received October 13, 2004

ABSTRACT: Oilfield formation damage by scale formation can occur when two incompatible brine streams are mixed. A common method for preventing scale formation is the use of chemical scale inhibitors such as aminotri-(methylene phosphonic acid) (ATMP). Scale inhibitors are injected and retained in the reservoir by adsorption and/or precipitation. The induction time, the period between the establishment of supersaturation and the detection of a new phase, is a measure of the ability of an inhibitor solution to remain in the metastable state. As a result, long induction times allow transport of inhibitor fluids into the near-wellbore regions without precipitation of the scale inhibitor and subsequent formation damage. In this study, an induction time model is applied to precipitation of the inhibitor (ATMP) with Ca^{2+} ions. The nucleation kinetics can be described by classical nucleation theory. Solution equilibrium was calculated by accounting for inhibitor dissociation and cation−inhibitor complexing as a function of ionic strength. Conditions such as the initial concentration of inhibitor, the solution pH, and the presence of soluble impurities significantly impact the precipitation kinetics of inhibitors. Long induction times were observed at low initial concentrations of inhibitor, at low values of the solution pH, and in the presence of impurities. Monovalent cation impurities (Li, Na, and K) inhibit the nucleation of Ca−ATMP to the same extent, indicating there is no effect on the different types of monovalent cations. Divalent cation impurities inhibit the nucleation of Ca−ATMP more than monovalent cations, and different divalent cations have different induction times. The reduction of nucleation rate is a result of increasing the surface free energy. This study provides an understanding of scale inhibitor precipitation kinetics which will be beneficial for delaying inhibitor precipitation in order to avoid reservoir permeability problems in near-wellbore region.

1. Introduction

Phosphonates have been used in several industrial applications for scale and corrosion control, such as crystal growth modifiers, dispersants, cleaning agents, and chelating agents. In oilfield application, phosphonates are used as scale inhibitors to prevent the formation of oilfield scales such as calcium carbonate, barium sulfate, and strontium sulfate. The precipitation of undesirable scale can cause serious problems in the petroleum industry, especially during the secondary oil recovery process. For offshore wells, seawater is pumped downhole to displace the petroleum. The water present in the reservoir, called the formation water, is often high in divalent cations (i.e., Ca, Mg, Ba, and Sr ions) which tend to form scale with sulfates or carbonates when mixed with the seawater. Scale formation can occur anywhere in the production system: around the wellbore surface, in porous formation, and on the surface of production equipment. If the scaling problem is not treated, continuous scale growth can eventually lead to blockage of the oil flow paths, damage to the production system, and a decrease in system productivity. When the production decreases to an unacceptable level due to scale blockage, the production system must be shut down in order to remove the scale. This cleanup costs oil producers millions of dollars per year due to productivity loss and overhaul expense.[1−4]

1.A. Scale Inhibitor Squeeze Treatments. Scale inhibitor squeeze treatments are commonly used techniques to manage reservoirs that have a high potential for scale formation. These treatments are carried out by squeezing (injecting) an inhibitor solution into the formation where the inhibitor is retained within the reservoir during the shut-in period. The subsequent release of inhibitor into the produced water after start-up provides protection against scale formation. Squeeze treatments are expensive due to the chemical costs, pumping costs, and most importantly lost production costs. The treatments are repeated when the inhibitor concentration in the produced water falls below the effective inhibition level (usually 1−20 ppm). Therefore, the success of squeeze treatments is often determined by the length of time known as the squeeze lifetime that is the time before the reservoir needs to be retreated with inhibitor.

The two most common industrial scale inhibitor squeeze-treatment techniques are identified by the retaining/releasing mechanisms of scale inhibitor within the formation. The first technique is the adsorption squeeze treatment, where the inhibitor is retained by adsorption onto the reservoir rock and is released by desorption. The second technique is the precipitation squeeze treatment, where the inhibitor is retained within the formation as a precipitate and is released

* To whom correspondence should be addressed. E-mail: sfogler@umich.edu.
† University of Michigan.
‡ Chulalongkorn University.

10.1021/cg049874d CCC: $30.25
Published on Web 12/08/2004

by dissolution.[5] Much of the field application research has focused on adsorption squeeze treatments, despite the fact that precipitation squeeze treatments offer longer squeeze lifetimes than conventional absorption squeeze treatments under comparable conditions.[6,7] Precipitation squeeze treatments are used less often than the absorption squeeze due to the concerns of formation blockage and damage caused by the precipitation of inhibitor in the near-wellbore region. However, success in scale formation control found in many oilfields is attributed to the precipitation squeeze treatments.[6] Therefore, great promise exists for precipitation squeeze treatments, although only a limited amount of research has been carried out to provide fundamental understanding of the reaction kinetics and mechanisms underpinning this treatment.

1.B. Scale Inhibitor Precipitation Squeeze Treatments. Precipitation squeeze treatments are carried out by squeezing (injecting) an aqueous inhibitor solution into the formation where the inhibitor is retained as a salt precipitate with divalent cations such as calcium ions. In sandstone formations, the inhibitor is injected into a calcium rich brine and the inhibitor precipitates spontaneously within the formation. On the other hand, in carbonate formations the inhibitor precipitate can be generated by reacting the acidic inhibitor with calcium contained in the rock formation. During inhibitor precipitation squeeze treatments, nucleation kinetics plays an important role in the spread of the inhibitor in the treatment zone as the injected fluid flows out into the formation. The slower precipitation would result in precipitate formation further away from the injection well. Generally, a mildly acidic solution of inhibitor can be used to obtain the inhibitor precipitation at several meters away from the wellbore.[8]

Although squeeze treatments are often used to control scale formation, their usage is based more on experience than on scientific understanding. It is unclear on where and how scale inhibitors precipitate during the injection of inhibitor solutions into the wellbore. Upon reviewing the literature, one finds the scientific explanations for the precipitation of scale inhibitors are not complete. The factors controlling inhibitor precipitation as well as the length of time before inhibitors precipitate from solution are still very difficult to predict. The chemical mechanisms of precipitation squeeze treatments are much less understood than those of the adsorption squeeze treatments. The main objective of this work is to provide a fundamental understanding of the precipitation kinetics of scale inhibitors in order to elucidate the actual squeeze treatments in the field. Each treatment is a highly complicated process, and each reservoir presents its own unique characteristics, such as formation water composition, temperature, or pressure. Our research aims to identify treatment variables and strategies in order to cause inhibitor precipitation to occur far away from the wellbore.

Phosphonates such as aminotri(methylene phosphonic acid) (ATMP) are commonly used inhibitors in the field. Some of the advantages they offer include the following: (a) their ability to inhibit scale at low concentrations, making them more economically viable than sequestrates such as EDTA; (b) their stability over a wide range of temperatures and pH values; (c) their ability to inhibit many different types of scale; and (d) the ease with which their concentration in the produced fluid can be determined. Hence, it is essential information to decide when a formation needs to be retreated. Because of these advantages, ATMP phosphonate scale inhibitor was used in this study.

Previous studies in our research group on precipitation squeeze treatments found that the solution pH is one of the most important factors affecting the molar ratio of Ca to ATMP in the precipitated solid.[1,9] As the precipitating solution pH increases, a greater number of hydrogen atoms deprotonate from the ATMP molecule. Consequently, the Ca ion has a greater number of reacting sites available on the ATMP molecule, resulting in an increased molar ratio of Ca to ATMP in the precipitate. It was found that the amount of Ca−ATMP precipitated increased with increasing solution pH: 78% precipitated at pH 1.5, 87% at pH 4, and 89% at pH 7. The dissolution rate of the precipitates formed at high pH values was much slower (0.03 μmol/cm^2 min for pH 7) than that of the precipitates formed at low solution pH values (2.38 μmol/cm^2 min for pH 1.5). The effectiveness of a scale inhibitor squeeze treatment is often measured by its lifetime.[9] The factors governing the treatment lifetime are the total amount of inhibitor retained in the formation, the retention/release mechanisms, and the location of the inhibitor within the reservoir.[10] Previous research has shown that the precipitation and subsequent dissolution of inhibitor precipitate from porous media enhance treatment lifetimes by increasing the amount of inhibitor retention and slowing the release characteristics of inhibitor retention during the production.[6] The amount of ATMP precipitated and the dissolution rate suggest that squeeze treatments at high pH solution will provide a longer squeeze lifetime compared to the lifetime at low pH. For example, the amount of precipitate at pH 7 was greater and the dissolution rate was slower when compared to results for precipitates formed at pH 1.5 as mentioned in a previous study.[9] However, the actual squeeze treatments are very complicated processes. Squeeze treatments with pH 7 brines containing ATMP and high Ca ions would generate a desirable precipitated product; however, the precipitation rate is rapid and as a result the precipitate would be located near the wellbore rather than far out into the formation.

1.C. Nucleation and Induction Time. During the past decade, measurements of the induction time have been used extensively to study the nucleation process. The induction time, t_{ind}, is frequently used to estimate the nucleation time and is defined as the time elapsed between the creation of a supersaturation solution and the first appearance of a new crystalline solid phase, ideally nuclei with the critical cluster size dimensions.[11] However, as the induction time is determined experimentally, it may also include growth to a detectable size once the nuclei are formed. If it is assumed that the nucleation time is much greater than the time required for growth of crystal nuclei to a detectable size, then the induction period is inversely proportional to the primary nucleation rate (J) as shown in eq 1:[12]

$$t_{ind} = \frac{1}{J} \tag{1}$$

The primary nucleation rate is represented by

$$J = A \exp\left[-\phi\beta \frac{\gamma^3 v^2}{(k_B T)^3 (\ln S)^2}\right] \quad (2)$$

where A is a frequency factor, ϕ is a factor for the energy barrier ($\phi = 1$ for homogeneous nucleation and $\phi < 1$ for heterogeneous nucleation), β is a shape factor, γ is the crystal surface energy, v is the molecular volume of the crystalline phase estimated by ACD/Chemsketch[13] to be 2.369×10^{-28} m^3 for Ca−ATMP, k_B is the Boltzmann constant, T is the absolute temperature (K), and S is the supersaturation ratio which is described in the solution equilibria calculation section. A correlation relating the induction time with the saturation level S is obtained by combining eqs 1 and 2:

$$\ln t_{ind} = \phi\beta \frac{\gamma^3 v^2}{(k_B T)^3 (\ln S)^2} + \ln\frac{1}{A} \quad (3)$$

The value of the surface energy γ can be extracted from the slope in a plot of ln t_{ind} as a function of [1/(ln S)^2]. The thermodynamic supersaturation ratio (S) for Ca−ATMP is defined by

$$S = \frac{[Ca^{2+}][ATMP^{2}]}{[Ca^{2+}]_{eq}[ATMP^{2-}]_{eq}} \quad (4)$$

where [Ca^{2+}] and [$ATMP^{2-}$] refer to concentrations of free Ca^{2+} and $ATMP^{2-}$ in solution while [Ca^{2+}]$_{eq}$ and [$ATMP^{2-}$]$_{eq}$ are the equilibrium concentrations. In this study, the equilibrium solubility was calculated from the activity product of Ca^{2+} and $ATMP^{2-}$ ions. The activities of Ca^{2+} and $ATMP^{2-}$ were calculated from total concentrations of Ca and ATMP in solution accounting for the formation of Ca−ATMP complex species in the liquid phase. Activities of Ca−ATMP complex were calculated as described in section 1.D. Activities of Ca^{2+} and $ATMP^{2-}$ were obtained after subtracting total activities of Ca and ATMP in the complex form from total Ca and ATMP in solution.

1.D. Acid−Base and Complexation Reactions. The prediction of the activity of each species in a solution of a polyprotic acid such as ATMP in the presence of complexing agents is a difficult task because the calculation requires numerous equilibrium constants.[14] ATMP is a weak polyprotic acid which does not completely dissociate in aqueous solution. The degree of ATMP protonation depends on pH, temperature (T), and ionic strength (I).[15] The protonation of ATMP (L) is composed of six steps and can be generalized as follows:

$$H_{i-1}L^{(n-i+1)-} + H^+ \rightarrow H_iL^{(n-i)-} \quad (5)$$

$$K_{a_i} = \frac{[H_iL^{(n-i)-}]}{[H_{i-1}L^{(n-i+1)-}][H^+]} \quad (6)$$

where n is the total number of deprotonated protons (for ATMP, $n = 6$), and i is the number of protons in the ATMP complex with H^+. The concentration of ATMP−H^+ complexes at different degrees of proton association, $H_iL^{(n-i)-}$, can be expressed in terms of the acid constant, K_{a_i}, the concentration of free inhibitor, L^{n-}, and H^+.

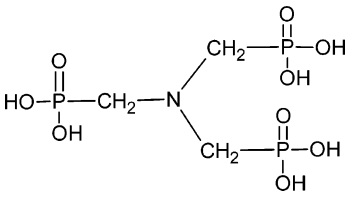

Figure 1. Chemical structure of ATMP.

$$[H_iL^{(n-i)-}] = \frac{[H^+][L^{n-}]}{K_{a_1}^N K_{a_2} \ldots K_{a_i}} \quad (7)$$

In the presence of Ca^{2+}, Ca−ATMP complexes are formed by the combination of Ca^{2+} and deprotonated ATMP in solution. The general reactions for the formation of Ca−ATMP complex and its equilibrium constant, K_{ij}, are given by

$$Ca_{j-1}H_iL^{(n-i-2(j-1))-} + Ca^{2+} \rightarrow Ca_jH_iL^{(n-i-2j)-} \quad (8)$$

$$K_{ij} = \frac{[Ca_jH_iL^{[n-i-2j]-}]}{[Ca^{2+}][Ca_{j-1}H_iL^{[n-i-2(j-1)]-}]} \quad (9)$$

where j is the number of Ca^{2+} associated with an ATMP molecule. To obtain activities of each component under diverse solution conditions, it is essential to know both the acid−base and complexation equilibrium constant. An electrostatic based model has been proposed for ATMP equilibrium constant calculation as shown below:

$$\log K = a + b|q| \quad (10)$$

where a and b are empirical constants determined from titration experiments and q is the absolute value of the charge on the inhibitor species that are being associated. The empirical equations used to calculate a and b for proton and Ca^{2+} ion association of ATMP are

$$a_{H^+} = 2.296 - 0.567\sqrt{I} + 0.184I - \frac{314}{T}$$

$$b_{H^+} = 1.439 - 0.160\sqrt{I} + 0.0255I - \frac{54.3}{T} \quad (11)$$

$$a_{Ca^{2+}} = 0 \qquad b_{Ca^{2+}} = 1.569 - 0.606\sqrt{I} + 0.201I - \frac{206}{T} \quad (12)$$

These empirical equations (eqs 11 and 12), which were obtained from the literature, were used to predict equilibrium constants.[15] The activities of Ca^{2+} and $ATMP^{2-}$ species used for supersaturation calculation in eq 4 were then calculated in a manner similar to that for DTPMP (diethylenetrinitrilopentakis(methylenephosphonic acid)) reactions as described in a previous study.[16]

2. Materials and Methods

2.A. Materials. A commercial grade ATMP (Dequest 2000) was obtained from Solutia. The ATMP molecule contains three active phosphate groups as shown in Figure 1. The salt solution used in the precipitating experiments was prepared from analytical grade reagents of $CaCl_2 \cdot 2H_2O$, LiCl, NaCl, KCl, and $MgCl_2 \cdot 6H_2O$ and ultrapure deionized water.

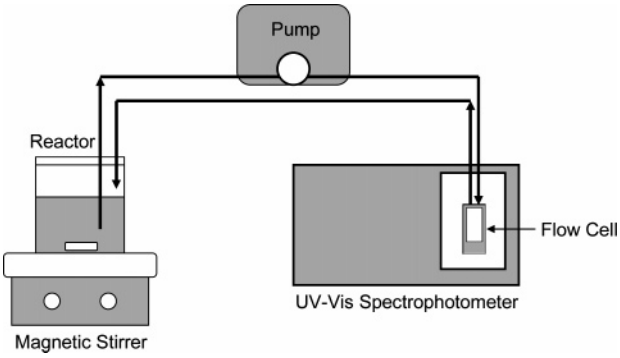

Figure 2. Experimental apparatus for precipitation experiments.

2.B. Induction Time Determination. The induction times of Ca−ATMP in various precipitating conditions were determined using the apparatus as shown in Figure 2.

All precipitation experiments were carried out at room temperature (25 °C). To establish a solution of Ca−ATMP, a desired amount of ATMP solution and deionized water were placed in a 250 mL glass reactor and stirred continuously by a magnetic stirrer. The pH was adjusted to the required value by addition of concentrated potassium hydroxide solution as needed. A $CaCl_2$ solution was then added to induce the supersaturation of Ca−ATMP in solution. Turbidity of the solution in terms of absorbance was monitored by circulating the solution through the quartz flow cell placed in the UV/vis spectrophotometer. The solution turbidity stayed constant for a certain period of time, and then an increase of turbidity was observed at the point where the precipitate was formed. The advantages of using turbidity for induction time measurements over more sophisticated methods, such as laser light scattering, are the low cost, availability, and ease of use of a spectrophotometer. Moreover, a spectrophotometer is more sensitive than visual detection of crystals with an optical microscope.[17] A typical plot of turbidity as a function of elapsed time for Ca−ATMP precipitation is shown in Figure 3a. The induction time, t_{ind}, is identified by the intersection with the elapsed time axis of the linear region of the plot of the change in absorbance over a 20 s time interval as a function of elapsed time as shown in Figure 3b. While other definitions of t_{ind} may exist, the trends in the variation of t_{ind} with the system variables will be the same (such as time to reach Abs = 0.01). After each run, tube and flow cell were rinsed with 1 M aqueous HCl solution and deionized water to remove residual precipitate. The precipitating solution was transferred to a closed flask.

2.C. Characterization of ATMP Precipitates and Supernatants. The resulting precipitate was filtered using a 0.22 micron filter membrane, washed with a small amount of deionized water, and dried at 70 °C, and the composition of precipitates was determined using an energy dispersive X-ray analyzer (EDX). The solution was left to stand for a week, after which the supernatant was removed by filtering through a 0.22 micron filter and the equilibrium concentration was determined by the ascorbic acid colorimetric method after UV/persulfate oxidation (Hach technique).

3. Results and Discussion

The effect of the solution pH on scale inhibitor precipitation was investigated at an initial ATMP concentration of 0.038 M and a Ca to ATMP molar ratio in solution of 1:1. Figure 4 shows the solution turbidity as a function of elapsed time after the $CaCl_2$ solution was added into the ATMP solution for solution pH values of 1.5 and 7.

The results show that the rate of precipitation of Ca−ATMP precipitates at pH 7 is much faster than at pH 1.5. At pH 7, a powdery 3:1 Ca−ATMP precipitate was formed immediately after the solutions of Ca and ATMP were mixed. At pH 1.5, a platelike 1:1 Ca−ATMP precipitate was formed and a longer time was required for precipitation. The results demonstrate the profound effect of solution pH on the rate of scale inhibitor precipitation. The squeeze treatments at pH 7 will result

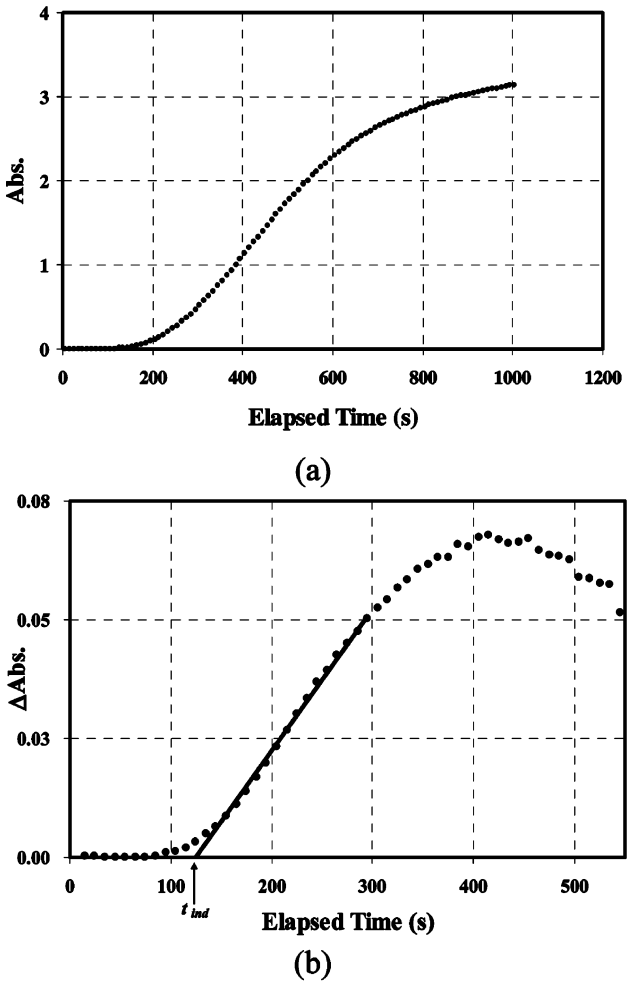

Figure 3. (a) Typical desupersaturation curves. (b) The value of absorbance difference ($\Delta Abs = Abs_t - Abs_{t-1}$) as a function of elapsed time, indicating t_{ind}.

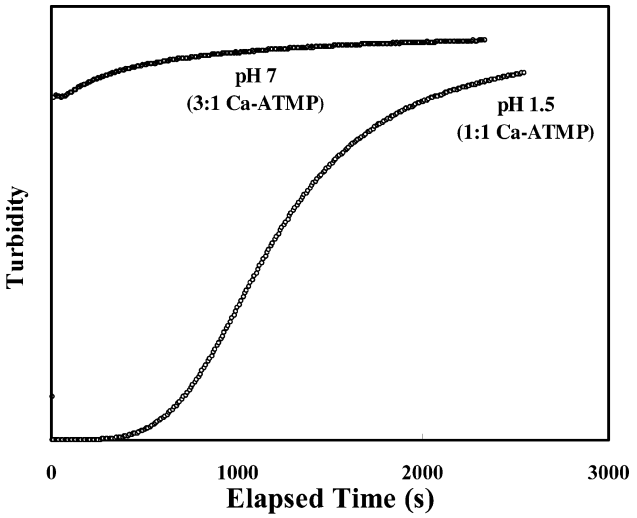

Figure 4. The effect of solution pH on the precipitation of Ca−ATMP precipitates.

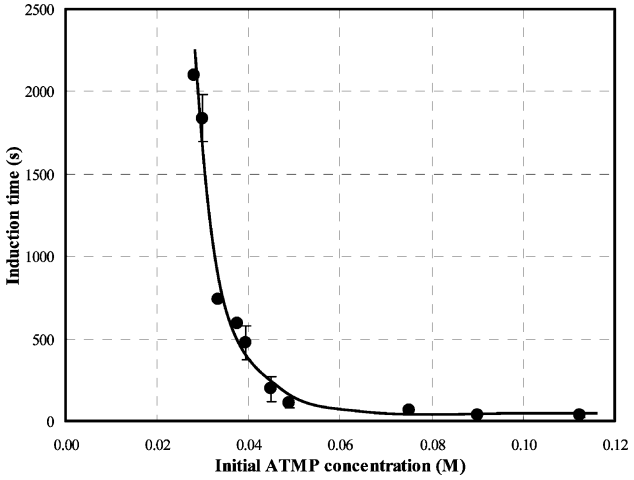

Figure 5. The plot of induction time as a function of initial concentration of ATMP.

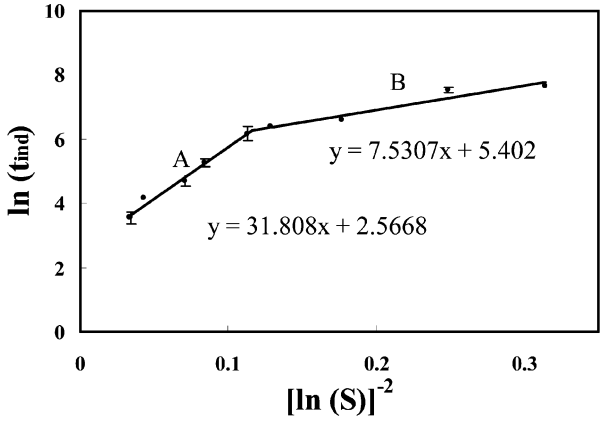

Figure 6. Induction periods as a function of initial supersaturation of Ca−ATMP. A = homogeneous, B = heterogeneous nucleation.

in the precipitation of inhibitor near the wellbore region, while slower precipitation and longer distance from the wellbore will be obtained at pH 1.5. The precipitation of scale inhibitor at pH 7 does provide the greater amount of inhibitor precipitated and a slower rate of dissolution. However, the quick precipitation of inhibitor might result in the formation damage and decrease of fluid conductivity near the wellbore region. While limited information on the placement of scale inhibitor precipitation can be found in the literature, one study on limestone confirmed that the distance from the wellbore at which scale inhibitor precipitation takes place is a significant factor that controls the return of scale inhibitor (or the squeeze lifetime of the treatments).[18] A greater distance from the wellbore would result in a longer squeeze lifetime. The precipitation of Ca−ATMP at pH 7 is very rapid, and the scale inhibitor precipitations are highly complex. For example, the precipitation of Ca−ATMP in the presence of Mg would result in the complex precipitation of (Ca+Mg)−ATMP in the system. Therefore, Ca−ATMP precipitation at pH 1.5 was investigated intensively in this study.

3.A. Precipitation of Ca−ATMP at pH 1.5. The precipitation kinetics of Ca−ATMP at pH 1.5 was studied in batch precipitation experiments for a range of initial concentrations of ATMP between 0.03 and 0.1 mol L^{-1}. A 1:1 molar ratio of Ca to ATMP in solution was used in all experiments. In the Ca−ATMP precipitation reaction

$$Ca^{2+} + ATMP^{2-} \rightarrow CaATMP(s) \qquad (13)$$

1 mol of Ca^{2+} precipitates with 1 mol of $ATMP^{2-}$ forming 1:1 Ca−ATMP precipitate. The Ca−ATMP precipitated as a white solid particle rather than a viscous phase as has been reported for the precipitation of polyacrylate inhibitor.[8] All the system variables (e.g., pH, concentration) remained constant during the induction period, which was confirmed by the withdrawal of samples through membrane filters for analysis of pH and ATMP concentrations.

It was found that induction time decreased with increasing initial concentration of ATMP as shown in Figure 5. For example, the induction time decreased from 2097 s (~35 min) to 95 s (~1.5 min) when the initial concentration of ATMP was increased from 0.028 M (0.84 wt %) to 0.112 M (3.3 wt %). The results suggest that the placement of inhibitor in the reservoir can be controlled by adjusting the concentration of ATMP in solution.

3.B. Surface Free Energy Calculation. The surface free energy of Ca−ATMP nucleation was calculated from the slope of the plot between $\ln(t_{ind})$ and $1/[\ln(S)]^2$ in the homogeneous nucleation region (line A) as shown in Figure 6. The supersaturation ratios were calculated accounting for acid−base and complexing reactions of ATMP and Ca ions as described in sections 1.C and 1.D. It was found that the data fall into two linear regions with two different slopes. These results suggest that the homogeneous nucleation (line A) holds only at a supersaturation ratio higher than 16.3 (i.e., small $[\ln(S)]^{-2}$). At a low supersaturation, precipitation is attributed to heterogeneous nucleation (line B). From eq 3, the surface free energy of Ca−ATMP precipitate was found to be 23.24 mJ/m^2.

3.C. Precipitation of Ca−ATMP in the Presence of Impurities. As mentioned earlier, the actual squeeze treatments are a highly complicated process. In the actual field applications, the scale inhibitor precipitation occurs in the presence of other salts from either seawater or formation water. The effect of other cations, especially in seawater and formation water, on scale inhibitor precipitation kinetics has been elucidated in this study. Monovalent cations such as Na, Li, and K contained in seawater or divalent cations such Mg, Sr, and Ba contained in formation water were found to influence the nucleation process of Ca−ATMP by changing solubility, increasing surface free energy, and consequently decreasing the nucleation rate as described below.

A recent study reported that the solubility of Ca−ATMP was found to decrease with the addition of monovalent cations due to the salting-out effect.[9] On the other hand, the solubility of Ca−ATMP increases with the addition of divalent cations due to the formation of the stable divalent cation−ATMP complexes in solution, corroborating the results from this previous study.[9] The presence of impurities has a significant effect on the equilibrium concentration of precipitate.

The induction time was measured in order to compare the nucleation rate of Ca−ATMP in the absence and

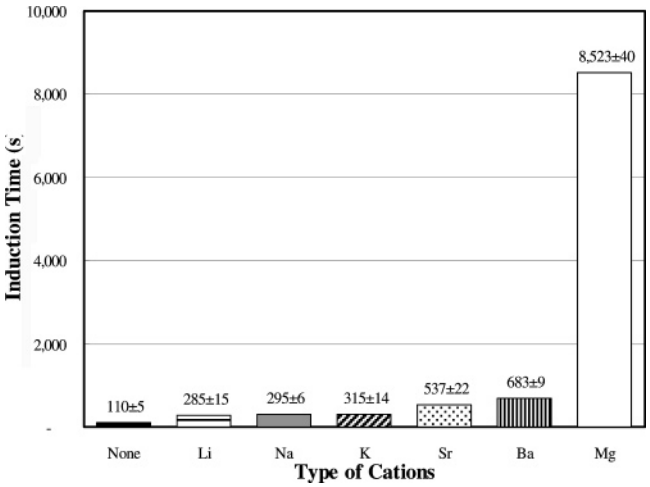

Figure 7. The induction time of Ca−ATMP precipitation in the presence of impurities.

presence of impurities. The effect of impurities on the induction time was studied using the same experimental procedure as that in the absence of impurities. The difference here is that the impurities (i.e., Li, Na, K, Mg, Sr, or Ba cations) in solution were added to ATMP solution prior to the addition of $CaCl_2$. The precipitation of Ca−ATMP in the absence of impurities was faster than in the presence. It is clear that the addition of other cations inhibits the nucleation of Ca−ATMP as indicated by the longer induction times, as the longer induction period indicates a greater inhibition of nucleation. Precipitates were formed as 1:1 Ca−ATMP precipitates in all experiments, and no impurities coprecipitated with Ca−ATMP precipitates.

Figure 7 shows the induction time in the absence and presence of cations at a solution pH of 1.5, an ATMP concentration of 0.045 M, and an impurity concentration of 0.05 M. Based on the induction time, all the monovalent cations studied appeared to inhibit the nucleation of Ca−ATMP to the same degree as evidenced by an increase by a factor of 2.75 in t_{ind}. The divalent cations (Ba, Sr, and Mg ions) were found to delay the nucleation of Ca−ATMP to a greater extent than the monovalent cations (Li, Na, and K ions). Different types of divalent cations appear to have a significant role in the efficiency of delaying the nucleation process of Ca−ATMP. Magnesium ions were found to have the greatest effect on inhibiting Ca−ATMP precipitation compared to Ba and Sr ions. However, the downside is that the amount of scale inhibitor precipitated will be diminished as mentioned in our previous study.[9]

The effect of Li, Na, K, and Mg ions (0.05 mol L^{-1}) on the surface free energy was investigated in solution at pH 1.5 and initial concentration of ATMP in the range of 0.024−0.098 mol L^{-1}. In the case of Mg, the formation of Mg−ATMP complex was accounted for using the equilibria calculations. The Mg−ATMP equilibrium constant was assumed to be equal to that for Ca−ATMP.[15] The addition of cations (e.g., Na, Li, K, and Mg ions) was found to increase the surface free energy of the nucleation. The effect of impurities on nucleation inhibition may be caused by adsorption or chemisorption on nuclei.[12] Values of the surface free energy calculated from eq 3, when impurities are present as the addition of Li, Na, K, and Mg ions, are shown in Table 1. In the presence of monovalent cations (e.g., Li, Na, and K ions), similar results were obtained with a slight difference in values of the surface free energy. The surface free energy was found to increase significantly to 33.51 mJ/m^2 by the addition of Mg to solution. This significant increase in the surface free energy in the presence of Mg may be due to the fact that Mg has a higher absorption strength of Mg on nuclei than that of monovalent cations and the fact that Mg may act as a structure-breaker in the solution phase. Our ongoing studies are directed toward further defining the precipitation kinetics of scale inhibitor in the presence of solid impurities contained in the reservoir such as sand, calcite, Barite, and various types of zeolite.

Table 1. Ca−ATMP Surface Free Energy in the Presence of Impurities

type of cation	surface free energy (mJ/m^2)
none	23.24 ± 0.21
Li	27.11 ± 1.38
Na	27.72 ± 0.85
K	27.79 ± 1.60
Mg	33.51 ± 0.52

4. Conclusions

1. The solution pH plays an important role in controlling the precipitation kinetics of Ca−ATMP.

2. The presence of impurities has a significant effect on the equilibrium concentration of the Ca−ATMP precipitate.

3. The addition of impurities inhibits the nucleation of Ca−ATMP as indicated by longer induction times.

4. Monovalent cation impurities (Li, Na, and K) inhibit the nucleation of Ca−ATMP to the same extent, indicating there is no effect on the different types of monovalent cations.

5. Divalent cation impurities inhibit the nucleation of Ca−ATMP more than monovalent cations, and different divalent cations have different induction times.

6. The order of nucleation inhibition is Li < Na < K < Sr < Ba < Mg.

7. The reduction of nucleation rate is a result of increasing the surface free energy.

8. The pH had both a positive and negative effect for uses in field applications. At a high pH, more Ca−ATMP is precipitated; however, the precipitation is relatively rapid and the precipitate is more likely to precipitate in the vicinity of the wellbore thereby reducing the effectiveness of the treatment.

9. The addition of Mg to the Ca−ATMP scale inhibitor system has two opposing effects for application in the field. The positive effect of adding Mg is that the precipitation is delayed so that the precipitate will be able to flow further out into the formation before precipitating. The negative effect is that less Ca−ATMP is precipitated when Mg is added, resulting in a shorter squeeze lifetime.

Acknowledgment. We express sincere gratitude for the financial support provided by the University of Michigan Porous Media Industrial Affiliates Program, including Baker Petrolite, Chevron Texaco, ConocoPhilips, Halliburton, PDVSA, Schlumberger, Shell Oil, and

Total Fina Elf, and the Thailand Research Fund under the Royal Golden Jubilee-Ph.D Program.

References

(1) Pairat, R.; Sumeath, C.; Browning, F. H.; Fogler, H. S. Precipitation and Dissolution of Calcium−ATMP Precipitates for the Inhibition of Scale Formation in Porous Media. *Langmuir* **1997**, *13*, 1791−1798.
(2) *Dequest Phosphonates*: *Introductory Guide*; Solutia: St. Louis, MO, 1998.
(3) Dunn, K.; Daniel, E.; Shuler, P. J.; Chen, H. J.; Tang, Y.; Yen, T. F. Mechanisms of Surface Precipitation and Dissolution of Barite: A Morphology Approach. *J. Colloid Interface Sci.* **1999**, *214*, 427−437.
(4) Allen, T. O.; Roberts, A. P. Scale Deposition, Removal, and Prevention. In *Production Operation*: *Well Completions, Workover, and Stimulation*; Oil & Gas Consultants: Tulsa, OK, 1989; Vol. 2, pp 245−255.
(5) Davies, K. G.; Hermann, B. P; Dohan, F. C.; Foley, K. T.; Bush, A. J.; Wyler, A. R.; Rabaioli, M. R.; Lockhart, T. P. Solubility and Phase Behavior of Polyacrylate Scale Inhibitors. *J. Pet. Sci. Eng.* **1996**, *15*, 115−126.
(6) Carlberge, Precipitation Squeeze Can Control Scale in High-volume Wells. *Oil Gas J.* **1983**.
(7) Browning, F. H.; Fogler, H. S. Precipitation and Dissolution of Calcium Phosphonates for the Enhancement of Squeeze Lifetimes. *SPE Prod. Facil.* **1995**, *10* (3), 144−150.
(8) Davies, K. G.; Hermann, B. P; Dohan, F. C.; Foley, K. T.; Bush, A. J.; Wyler, A. R.; Rabaioli, M. R.; Lockhart, T. P. Solubility and Phase Behavior of Polyacrylate Scale Inhibitors. *J. Pet. Sci. Eng.* **1996**, *15*, 115−126.
(9) Tantayakom, V.; Fogler, H. S.; de Moraes, F. F.; Bualuang, M.; Chavadej, S.; Malakul, P. Study of Ca−ATMP Precipitation in the Presence of Magnesium Ion. *Langmuir* **2004**, *20* (6), 2220−2226.
(10) Andrei, M.; E. B.; Lockhart, T. P. Phase Behaviour of Phosphinopolyacrylate Scales Inhibitor. *J. Dispersion Sci. Technol.* **1999**, *20* (1&2), 59−81.
(11) Siobbhan, F. E.; Boerlage, M. D. K.; Bremere, I.; Witkamp, G. J.; Van der Hoek, J. P.; Schippers, J. C. The Scaling Potential of Barium Sulphate in Reverse Osmosis Systems. *J. Membr. Sci.* **2002**, *197*, 251−268.
(12) Mullin, J. W. *Crystallization*, 3rd ed.; Butterworth Heinemann: Oxford, 1997.
(13) *ACD/ChemSketch*; Advanced Chemistry Development Inc.: Toronto, Ontario, Canada, 2002.
(14) Butler, J. N. *Ionic Equilibrium*: *Solubility and pH Calculations*; Wiley: New York, 1998.
(15) Kan, A. T.; Fu, G.; Al-Thubaiti, M.; Xiao, J.; Tomson, M. B. *A New Approach to Inhibitor Squeeze Design.* In *SPE International Symposium on Oilfield Chemistry*, Houston, TX, 2003: Society of Petroleum Engineers: Dallas, TX, 2003.
(16) Tomson, M. B.; Kan, A. T.; Oddo, J. E. The Acid/Base and Metal Complex Solution Chemistry of the Polyphosphonate, DTPMP Versus Temperature and Ionic Strength. *Langmuir* **1994**, *10*, 1442−1449.
(17) Hu, H.; Yang, X.; Wilson, L. J. A Spectrophotometer-based Method for Crystallization Induction Time Period Measurement. *J. Cryst. Growth* **2001**, *232*, 86−92.
(18) Essel, A. J.; Carlberg, B. L. Strontium Sulfate Scale Control by Inhibitor Squeeze Treatment in the Fateh Field. *J. Pet. Technol.* **1982**, *34* (6), 1302−1306.

CG049874D